FRIGID ZONE **MEDICINE**
Original Article • DOI: 10.2478/fzm-2024-0006

YBX1 inhibits mitochondrial-mediated apoptosis in ischemic heart through the PI3K/AKT signaling pathway

Fangfang Bi[1#], Miao Cao[1#], Yuquan Wang[1], Qingming Pan[1], Zehong Jing[1], Danyang Bing[1], Lifang Lyu[1], Tong Yu[2], Tianyu Li[1], Xuelian Li[1], Haihai Liang[1], Hongli Shan[2*], Yuhong Zhou[1,3*]

Abstract

Background: Myocardial infarction (MI) is associated with higher morbidity and mortality in the world, especially in cold weather. YBX1 is an RNA-binding protein that is required for pathological growth of cardiomyocyte by regulating cell growth and protein synthesis. But YBX1, as an individual RNA-binding protein, regulates cardiomyocytes through signaling cascades during myocardial infarction remain largely unexplored. **Methods:** In vivo, the mouse MI model was induced by ligating the left anterior descending coronary artery (LAD), and randomly divided into sham operation group, MI group, MI+ YBX1 knockdown/overexpression group and MI+ negative control (NC) group. The protective effect of YBX1 was verified by echocardiography and triphenyltetrazolium chloride staining. In vitro, mitochondrial-dependent apoptosis was investigated by using CCK8, TUNEL staining, reactive oxygen species (ROS) staining and JC-1 staining in hypoxic neonatal mouse cardiomyocytes (NMCMs). **Results:** YBX1 expression of cardiomyocytes was downregulated in a mouse model and a cellular model on the ischemic condition. Compared to mice induced by MI, YBX1 overexpression mediated by adeno-associated virus serotype 9 (AAV9) vector reduced the infarcted size and improved cardiac function. Knockdown of endogenous YBX1 by shRNA partially aggravated ischemia-induced cardiac dysfunction. In hypoxic cardiomyocytes, YBX1 overexpression decreased lactic dehydrogenase (LDH) release, increased cell viability, and inhibited apoptosis by affecting the expression of apoptosis related proteins, while knockdown of endogenous YBX1 by siRNA had the opposite effect. Overexpression of YBX1 restored mitochondrial dysfunction in hypoxic NMCMs by increasing mitochondrial membrane potential and ATP content and decreasing ROS. In hypoxic NMCMs, YBX1 overexpression increased the expression of phosphorylated phosphatidylinositol 3 kinase (PI3K)/AKT, and the anti-apoptosis effect of YBX1 was eliminated t by LY294002, PI3K/AKT inhibitor. **Conclusion:** YBX1 protected the heart from ischemic damage by inhibiting the mitochondrial-dependent apoptosis through PI3K/AKT pathway. It is anticipated that YBX1 may serve as a novel therapeutic target for MI.

Keywords

YBX1; PI3K/AKT; apoptosis; mitochondrial function; myocardial infarction

Received 22 November 2023, accepted 22 January 2024

[1]*Department of Pharmacology (State-Province Key Laboratories of Biomedicine-Pharmaceutics of China, Key Laboratory of Cardiovascular Research, Ministry of Education), College of Pharmacy, Harbin Medical University, Harbin 150081, China*
[2]*Shanghai Frontiers Science Research Center for Druggability of Cardiovascular noncoding RNA, Institute for Frontier Medical Technology, Shanghai University of Engineering Science, Shanghai 201620, China*
[3]*Department of Basic Medicine, Xiamen Medical College, Xiamen 361023, China*

**Corresponding authors Yuhong Zhou, E-mail: zyh2023@xmmc.edu.cn; Hongli Shan, E-mail: shanhl@sues.edu.cn*
[#]These authors contributed equally to the manuscript.

1 Introduction

Myocardial infarction (MI) is associated with higher morbidity and mortality in the world[1] and is often accompanied by heart failure, arrhythmia, shock and even sudden death[2-3]. Cold exposure is one of the most important risk factors for MI. Cold exposure induced an oxidative stress and apoptosis in the myocardium leading to ventricular dysfunction[4-6]. Exploring the pathogenesis of MI and finding new therapeutic targets has always been an important research topic in the cardiovascular field.

Apoptosis is referred to the programmed death of cells and

induced by hypoxia and oxidative stress during MI[7]. Apoptosis triggers biochemical events such as cell contraction, rupture of the nucleus, and chromosome DNA damage[8]. Calcium overload in mitochondria during myocardium ischemia causes mitochondrial swelling and impaired membrane communication. The permeability of mitochondria increases, and Cytochrome C, a pro-apoptosis factor in mitochondria, is released into the cytoplasm, triggering the formation of apoptosome, and the promoter pro-caspase-9 is recruited into its caspase recruitment domain (CARD), caspase-3 and proteolysis are activated. It finally leads to apoptosis and death[9-10]. Inhibition of apoptosis is essential to protect the heart from ischemic damage. However, the complex mechanism of apoptosis induced by myocardial infarction remains unclear.

Y-box binding protein-1 (YBX1), as a DNA and RNA binding protein, regulates transcription and translation, mRNA pre-splicing, and a number of other cellular processes[11]. YBX1 is a classical oncogene which inhibits apoptosis in many cancers[12-14]. However, only a few studies have been done about the regulation of YBX1 on cardiac function. YBX1 silencing inhibited the metastasis of miR-133 and reduces the angiogenesis and endothelial-mesenchymal transition of fibroblasts[15]. CircNfix downregulation promoted cardiomyocyte proliferation and angiogenesis by degrading YBX1 ubiquitination and suppressing cyclin A2 and cyclin B1 expression in MI[16]. Long non-coding RNA Aerrie (linc01013) associates with YBX1 and regulate DNA damage signaling and repair in aging process of cardiovascular diseases[17]. YBX1 binds to eucaryotic elongation factor 2 (Eef2) mRNA and regulates global protein translation during cardiac hypertrophy[18]. RNA-protein interactions are important to regulate cardiac function, but YBX1, as an individual RNA-binding protein, how to regulate through signaling cascades in cardiomyocytes during MI is largely unknown.

Our study found that YBX1 was down-regulated in hypoxic cardiomyocytes and in MI heart. YBX1 plays an important role in MI and its underlying molecular and cellular mechanisms need to be elucidated. We observed the cardiac function, mitochondrial function and apoptosis by gain or loss function of YBX1 *in vivo* and *in vitro* experiment.

2 Materials and methods

2.1 Experimental animals and mouse model of MI

C57BL/6 male mice (18-22 g) were purchased from Changsheng Biotechnology (Liaoning, China) and maintained in cages under standard conditions according to the regulations of the Institutional Animal Care and Use Committee of Harbin Medical University.

The left anterior descending branch (LAD) of the mouse coronary artery was ligated to construct a model of myocardial infarction, following the previously described procedure[3]. A gas chamber with 2-4% isoflurane (MIDMARK, USA) was used to anesthetize mice and ventilate them *via* orotracheal intubation. A left thoracotomy was performed to expose the heart and LAD was ligated using a 7-0 suture. The mice in the sham group underwent the same procedure except for LAD ligation.

2.2 Virus vector construction and infection

We used adeno-associated virus serotype 9 vector (AAV9) to construct YBX1 knockout or YBX1 overexpression model *in vivo*. AAV9 vectors carrying a short RNA fragment for silencing YBX1 (shYBX1) and CAG promoter conjugated with green fluorescent protein (GFP) were constructed (Leder biological technology Co., Ltd., Guangzhou, Guangdong, China). The interference sequences were as following: Forward 5'CCGGGAGAACCCT AAACCACAAGATCTCGAGATCTTGTGGTTTAGGGTTCTCT TTTTT3' and Reverse 5'AAAAAAGAGAACCCTAAACCACAA GATCTCGAGATCTTGTGG TTTAGGGTTCTCCCGG3'. AAV9 vector carrying YBX1 sequence and enhanced GFP gene for YBX1 overexpression (AAV9- YBX1) was constructed. AAV9-YBX1 (1.3×10^{11}) was injected into the tail vein, and the mice were anesthetized 3 weeks after administration, and euthanized through neck amputation.

2.3 Echocardiography

Cardiac function of the mice was evaluated 6 hours after LAD ligation. The mice were anesthetized with pentobarbital (90 mg/kg, P3761, Sigma-Aldridge). Echocardiography was performed in M-mode with Vevo2100 high-resolution ultrasound imaging system (VisualSonics, Toronto, Ontario, Canada). ST-segment elevation in electrocardiogram (ECG) was used as an indicator of successful occlusion of the artery.

2.4 TTC staining

Myocardial tissue was immediately frozen and cut into 2-mm cross sections, followed by incubation in 2% TTC solution at 37°C for 20 minutes in the dark. Images were captured using a microscope.

2.5 TUNEL staining

Apoptosis was evaluated by the In Situ Cell Death Detection Kit (Roche, Mannheim, Germany). After TUNEL staining, the nuclei were counterstained with DAPI (Biosharp, Hefei, China). The TUNEL-positive cells were observed under a fluorescence microscope (Zeiss, Jena, Germany), and the ratio of TUNEL-positive cells over DAPI-positive nuclei was calculated.

2.6 Quantitative real-time PCR (qRT-PCR)

qRT-PCR was performed as previously described[3], using SYBR Green I (04913914001; Roche, Basel, Basel-City, Switzerland) to quantify target mRNA levels. α-actin was used as a reference gene. The sequences of qPCR primer pairs are: YBX1, forward 5'-AAGGTCATCGCAACGAAGGTT-3' and reverse 5'- CAAATACGTCTTCCTTGGTGCA-3'; GAPDH: forward 5'-GGGCTCGGCTCTCTCCTCCCTG-3', reverse 5'-TCCACCACCCAGTTGCTCTA-3'.

2.7 Culture of neonatal mouse cardiomyocytes (NMCMs) and hypoxia induction

For isolation of myocardial cells, the heart was quickly dissected out from 3-day-old newborn mice, ventricular myocardium was cut into small pieces, digested with 0.25% trypsin at 37°C until the tissue disappeared. The cell suspension was collected by centrifugation at 500 g for 5 minutes, and the collected cells were resuspended in a medium supplemented with 10% fetal bovine serum (Biological Industries, Kibbutz BeitHaemek, Israel), penicillin (100 U/mL), and streptomycin (100 U/mL; Beyotime, China) and cultured in a humid incubator with 5% CO_2 and 95% air at 37°C. After 90 minutes, the fibroblasts were removed. Dissociated cardiomyocytes were collected and plated onto 6-well plate for another 48 hours before being used in subsequent experiments. Cultured cardiomyocytes were incubated for 12 hours under anoxic conditions (5% CO_2 and 95% N_2) to simulate myocardial infarction *in vitro*.

2.8 Immunofluorescence staining

NMCMs were fixed in 4% paraformaldehyde and blocked with 10% goat serum, and cells and sectioned tissue specimens were stained with anti-YBX1 (1∶300) overnight, followed by incubation with a conjugated secondary antibody for 1 hour. Nuclei were stained with DAPI for 10 minutes prior to examinations under a fluorescence microscope (Olympus, IX73, Japan).

2.9 Transfection of siRNAs or plasmids to cells

YBX1-specific siRNA (siYBX1) and negative control siRNA (NC) were synthesized by Ribobio (China, Guangdong, Guangzhou). These constructs were transfected into NMCMs to knock down YBX1 at a final concentration of 100 nM. The sequence of siYBX1 is 5'-GGTGCAGGAGAGGAAGGTA-3'. YBX1 plasmids were constructed by Leder biological technology Co., Ltd., (Guangzhou, Guangdong, China). The pcDNA3.1 (+) empty vector was used as a negative control. NMCMs were transfected with corresponding siRNAs (100 nmol/L) or plasmids (200 ng/mL) for 48 hours (for protein analysis) or 24 hours (for RNA) and then exposed to hypoxia. X-treme Gene siRNA transfection reagent (Roche, Basel, Switzerland) was used for transfection of siRNAs, and Lipofectamine2000 (lipo2000) transfection reagent (Invitrogen, Carlsbad, USA) was utilized for overexpression plasmids. The scramble sequences and the empty plasmids were transfected as negative controls, respectively. In the control group, the cells were treated with the isochoric transfection reagent (lipo2000 or X-treme) only. Cardiomyocytes in the test group were treated with LY294002 (10 mmol/L; Cat00342, Proreintech, Wuhan, China) for 6-8 h.

2.10 Detection of mitochondrial membrane potential

The mitochondrial membrane potential assay kit with JC-1 (C2006, Beyotime, Shanghai, China) was used to assess the mitochondrial membrane potential of NMCMs, according to the manufacturer's protocol. After incubation with JC-1 staining solution for 20 minutes, the cardiomyocytes were examined under a fluorescence microscope (Olympus, IX73, Japan).

2.11 Cell viability

CCK8 assay was employed for cell viability CCK-8 (CK04-500T; Dojindo Laboratories Inc., Japan). The optical density of 450 nm was quantified using the absorbance values.

2.12 ATP production

ATP content in cells was detected using the ATP detection kit (S0026, Beyotime, Shanghai, China) according to the manufacturer's requirements. RLU values were measured using a photometer. The concentrations of ATP in the samples were determined based on the standard curve.

2.13 Determination of reactive oxygen species (ROS) generation

Intracellular ROS levels were measured using a Reactive Oxygen Species Assay Kit (S0033S, Beyotime, Shanghai, China). Briefly, the cells were plated into 24-well plates pretreated with DCFH-DA for 25 min at 37°C. Subsequently, the cells were observed using fluorescence microscopy (Zeiss, Jena, Germany) at a wavelength of 488 nm.

2.14 Western blot analysis

Protein levels in mouse ventricular tissues and neonatal cardiomyocytes were analyzed using Western blot analysis. The tissue specimens and primary cardiomyocytes were ground and lysed in a lysis buffer solution (RIPA: PI = 100∶1, Beyotime, China) on ice for 30 minutes, followed by centrifugation for 20 minutes (4°C, 13500 rpm/min). An equal amount of (60 μg)

protein samples from each group was fractionated by 10%/12% SDS-PAGE and electroblotted onto nitrocellulose membranes (Pall, New York, USA). Membranes were incubated with primary antibodies overnight at 4°C, including rabbit anti-YBX1antibody (Abcam, UK, Cat#: ab19867, 1 : 500), rabbit anti-Bcl-2 antibody (Proteintech, Wuhan ,China Cat#: 26293-1-AP, 1 : 500), rabbit anti-Bax antibody (Proteintech, Wuhan ,China, Cat#: 50599-2-AP, 1 : 500), rabbit anti-casapse-3 antibody (Proteintech, Wuhan, China, Cat#: 19677-1-AP, 1 : 500), and rabbit anti-casapse-9 antibody (Proteintech, Wuhan ,China,. Cat#: 10380-1-AP, 1 : 500). Mouse GAPDH antibody (Zhongshanjinqiao, Beijing, China, Cat#: TA-09, 1 : 1000) was used as an internal reference. The Odyssey v1.2 software was used to quantify blots (LICOR Biosciences, Lincoln, NE, USA).

2.15 Statistical analysis

Two-tailed Student's *t*-test was performed for comparisons between two groups, and one-way ANOVA with post hoc Tukey's test was used to compare the differences among multiple groups. *P* value less than 0.05 indicated statistical significance. The data are presented as mean ± SEM. All statistical analyses were carried out using GraphPad Prism 8.0 (GraphPad Software Inc., San Diego, USA).

3 Results

3.1 YBX1 expression is decreased in ischemic heart and hypoxic cardiomyocytes.

YBX1 microarray data related to ischemic heart were obtained from GEO database (http://www.ncbi.nlm.nih.gov/GEO) to explore its role in MI. In MI, YBX1 expression was significantly lower than in Sham (Fig. 1A and 1B). YBX1 has been reported to be involved in protein pathophysiology during MI. To evaluate the potential role of YBX1, a MI mouse model was constructed with LAD

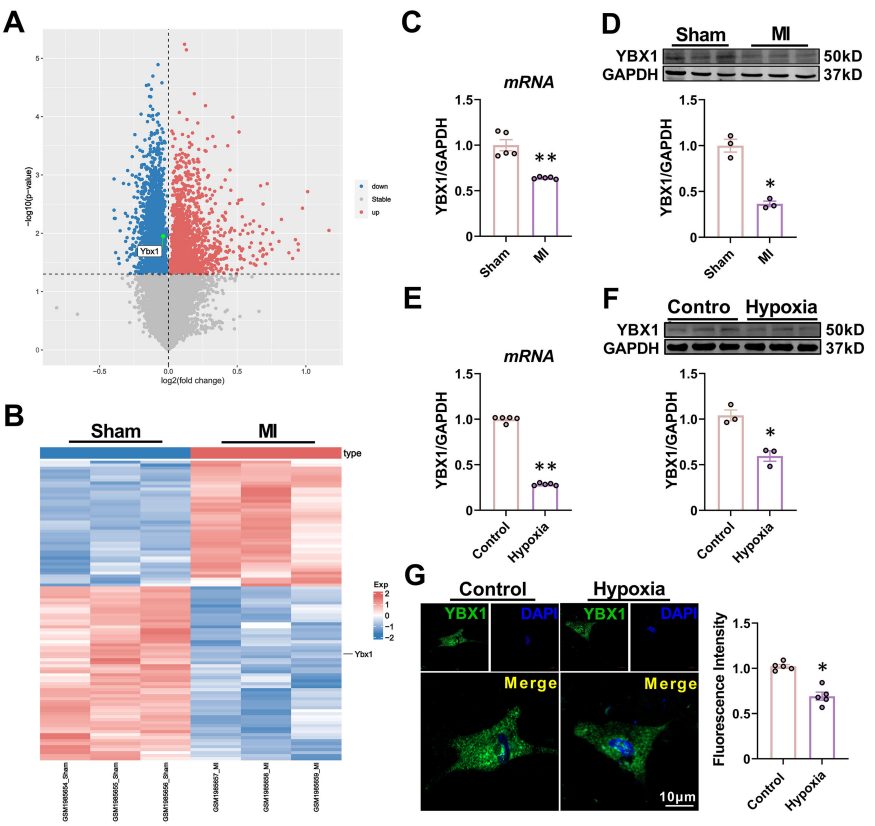

Fig. 1 YBX1 is downregulated in ischemic hearts and hypoxic cardiomyocytes. (A) Volcano plot of differentially expressed mRNAs from the GEO database (http://www.ncbi.nlm.nih.gov/geo), showing markedly downregulated YBX1 expression in MI mice compared to the Sham group. (B) The hierarchical clustering heat map. (C, D) YBX1 levels determined by RT-PCR and Western blot. $^{*}P < 0.05$, $^{**}P < 0.01$, $N = 3$-5 duplicates/group. (E, F) Downregulation of mRNA and protein levels of YBX1 in cultured neonatal mouse cardiomyocytes (NMCMs) after hypoxia treatment for 12 h relative to cells cultured under normoxic conditions. $^{*}P < 0.05$, $^{**}P < 0.01$, $N = 3$-5 duplicates/group. (G) Immunofluorescence displaying the changes of YBX1 expression and subcellular distribution (YBX1 in green, nucleus in blue). Scale bars: 10 μm. $^{*}P < 0.05$, $N = 5$ duplicates/group. The data are presented as mean ± SEM.

ligation. The presence of ST-segment elevation in the ECG and sudden local pallor of the myocardium were used as indicators of ischemia (Supplemental Fig. 1). After 6 hours, the expression of YBX1 RNA and protein was detected in cardiac infarction marginal tissue. Compared with sham group, the level of mRNAs of YBX1 in MI group decreased significantly (Fig. 1C). In addition, the protein level of YBX1 in MI group also decreased to 0.36 ± 0.05 (Fig. 1D, $P < 0.05$). Consistently, YBX1 mRNA and protein expression levels were also down-regulated in hypoxic NMCMs (Fig. 1E and 1F). Immunofluorescence results showed a punctate distribution of YBX1 (green) throughout the whole cell and down-regulation of YBX1 in hypoxic cardiomyocytes, as indicated by reduced green signals (Fig. 1G).

3.2 YBX1 improves heart function in MI mice

YBX1 expression was down-regulated in mouse MI model and in cellular hypoxia model, suggesting that YBX1 may play a crucial role in cardiac function under physiological conditions, suggesting an alleviation of damaged cardiac function by exogenous YBX1. Then, we used AAV9 vector containing YBX1 gene to detect whether it has a protective effect against ischemic heart injury (Fig. 2A). Overexpression of YBX1 by AAV9-Ybx1 was verified (Supplemental Fig. 2). As shown in Fig. 2B-2D, there was a significant decrease in cardiac function in the MI group, with reduced left ventricular ejection fraction (EF) and shorter fraction (FS) compared to the Sham group. Overexpression of YBX1 partially restored the depressed EF and FS in MI, EF of mice overexpressing YBX1 increased from 66.05 ± 3.75% to 72.50 ± 2.11% (Fig. 2C, $P < 0.05$), FS increased from 32.74 ± 5.93% to 39.68 ± 5.32% (Fig. 2D, $P < 0.05$). The NC construct (empty vector) failed to affect the ischemia-induced cardiac dysfunction. In addition, YBX1 overexpression mitigated the increases in LV anterior wall thickness and dilation, which was

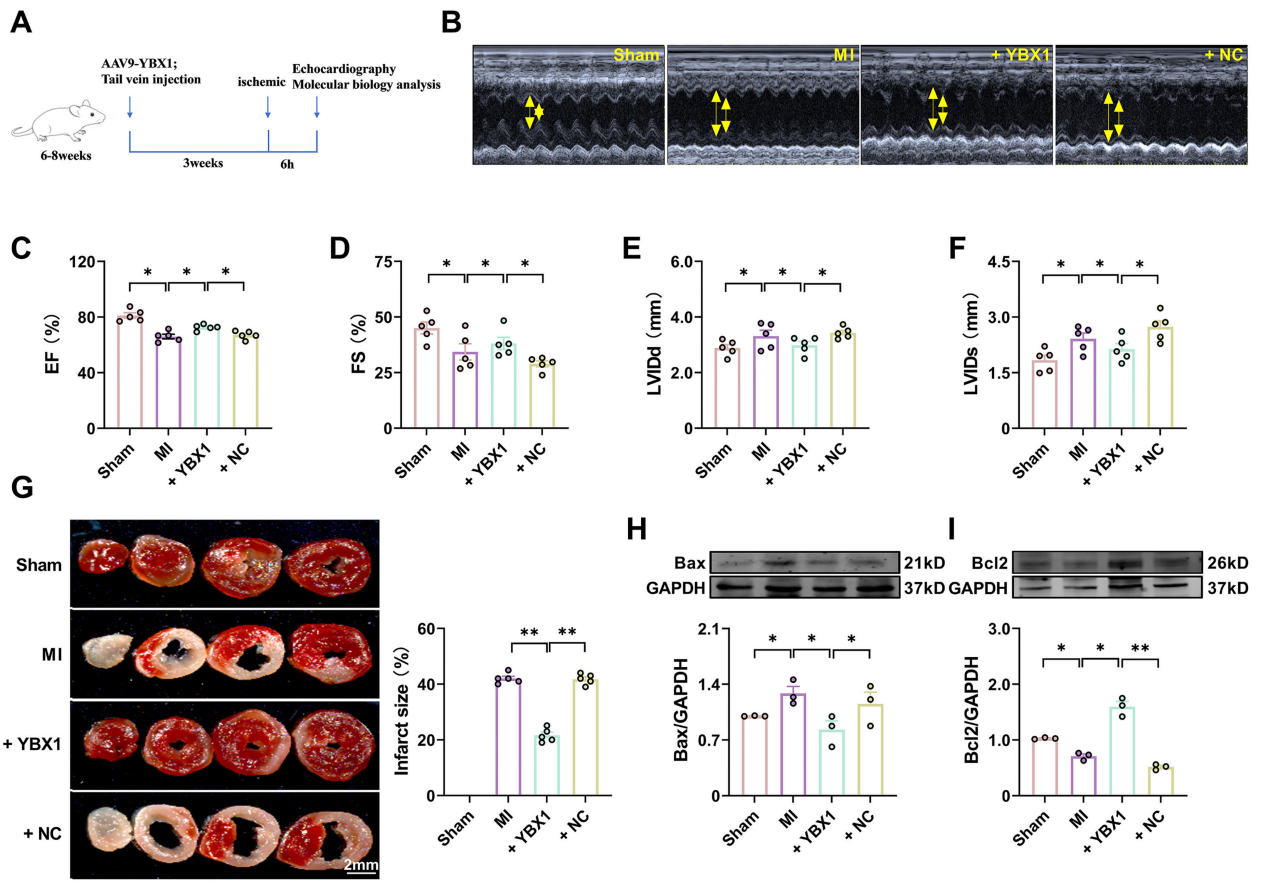

Fig. 2 Overexpression of YBX1 improves cardiac function in myocardial infarction (MI) mice. YBX1 was overexpressed by an AAV9 vector engineered to contain the full-length YBX1 gene in MI mice. (A) Experimental procedure. (B) Echocardiographic analysis of left ventricular dimensions and cardiac function in mice. (C) EF: ejection fraction (D) FS: fractional shortening of left ventricular diameter. (E) LVIDs: systolic left ventricular internal diameters. (F) LVIDd: diastolic left ventricular internal diameters. $^{*}P < 0.05$, $N = 5$. (H) TTC staining. $^{**}P < 0.01$, $N = 5$ duplicates/group. (H, I) Representative bands and statistical data on Bax and Bcl-2 expression, as determined by Western blot analysis. $^{*}P < 0.05$, $^{**}P < 0.01$, $N = 3$ duplicates/group.

reflected by decreased left ventricular diameter (LVIDd) at the end of diastole stage and left ventricular diameter (LVIDs) at the end of systole stage (Fig. 2E and 2F). Infarction size was enlarged and Bax expression was increased in MI mice, alongside decreased Bcl-2 expression, while YBX1 overexpression reduced the infarction size (Fig. 2G) and the expression of Bax and increased the expression of Bcl-2(Fig. 2H and 2I).

These results suggest that YBX1 protects the heart from ischemic damage. Next, we wanted to assess whether YBX1 knockdown is harmful to the heart. To this end, we utilized a loss-of-function approach with an AAV9 vector carrying an YBX1 shRNA fragment (shYBX1) and investigated the effects of YBX1 on heart function. The efficiency of YBX1 knockout was verified (Supplemental Fig. 3). As expected, shYBX1, but not the negative control (NC), significantly exacerbated the cardiac dysfunction during MI, as indicated by the reduced EF and FS (Fig. 3C and 3D), enlarged infarct size (Fig. 3G), elevated Bax expression, and diminished Bcl-2 expression, compared to non-treated MI mice (Fig. 3H and 3I).

3.3 YBX1 inhibits mitochondria-dependent apoptosis in cardiomyocytes under hypoxia.

To further verify the protective effect of YBX1 against ischemic injury, we investigated the effect of YBX1 on NMCMs cultured under hypoxic conditions. The mRNA and protein levels of YBX1 in the overexpression group were assessed to confirm the transfection efficiency (Supplemental Fig. 4). Many factors such as hypoxia can induce apoptosis, which is an evolutionarily conservative form of cell death[19]. Hypoxia decreased the viability of myocardial cells and increased the release of lactic

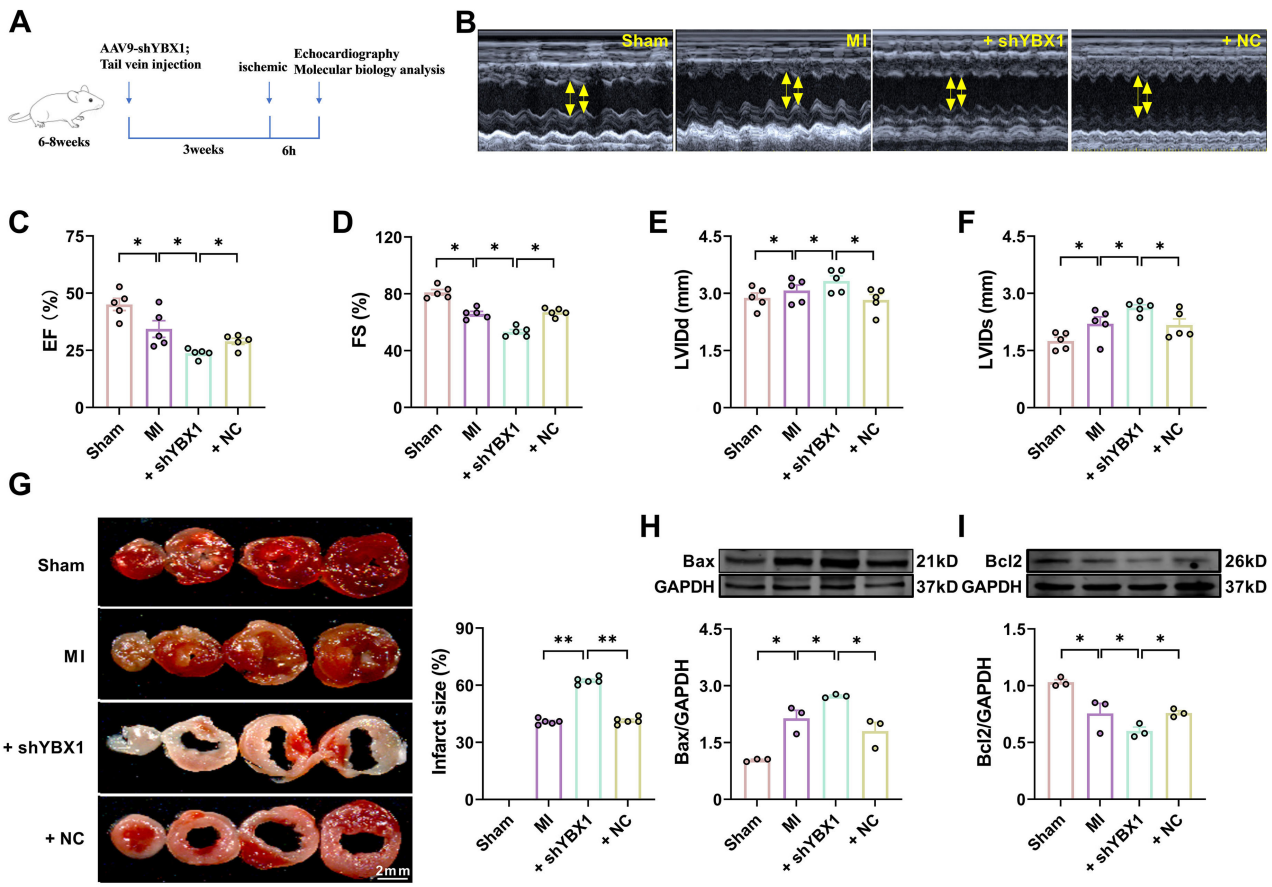

Fig. 3 Knockdown YBX1 aggravates cardiac dysfunction in myocardial infarction (MI) mice. YBX1 was knocked down *via* an AAV9 vector carrying a YBX1-specific shRNA in mice. (A) Experimental procedure. (B) Echocardiographic analysis of left ventricular dimensions and cardiac function in mice. (C) EF: ejection fraction (D) FS: fractional shortening of left ventricular diameter. (F) LVIDs: systolic left ventricular internal diameters. (F) LVIDd: diastolic left ventricular internal diameters. $^{*}P < 0.05$, $N = 5$. (G) Representative images of TTC staining. $^{**}P < 0.01$, $N = 5$ duplicates/group. (H, I) Representative bands and statistical data on Bax and Bcl-2 expression, as determined by Western blot analysis. $^{*}P < 0.05$, $N = 3$ duplicates/group.

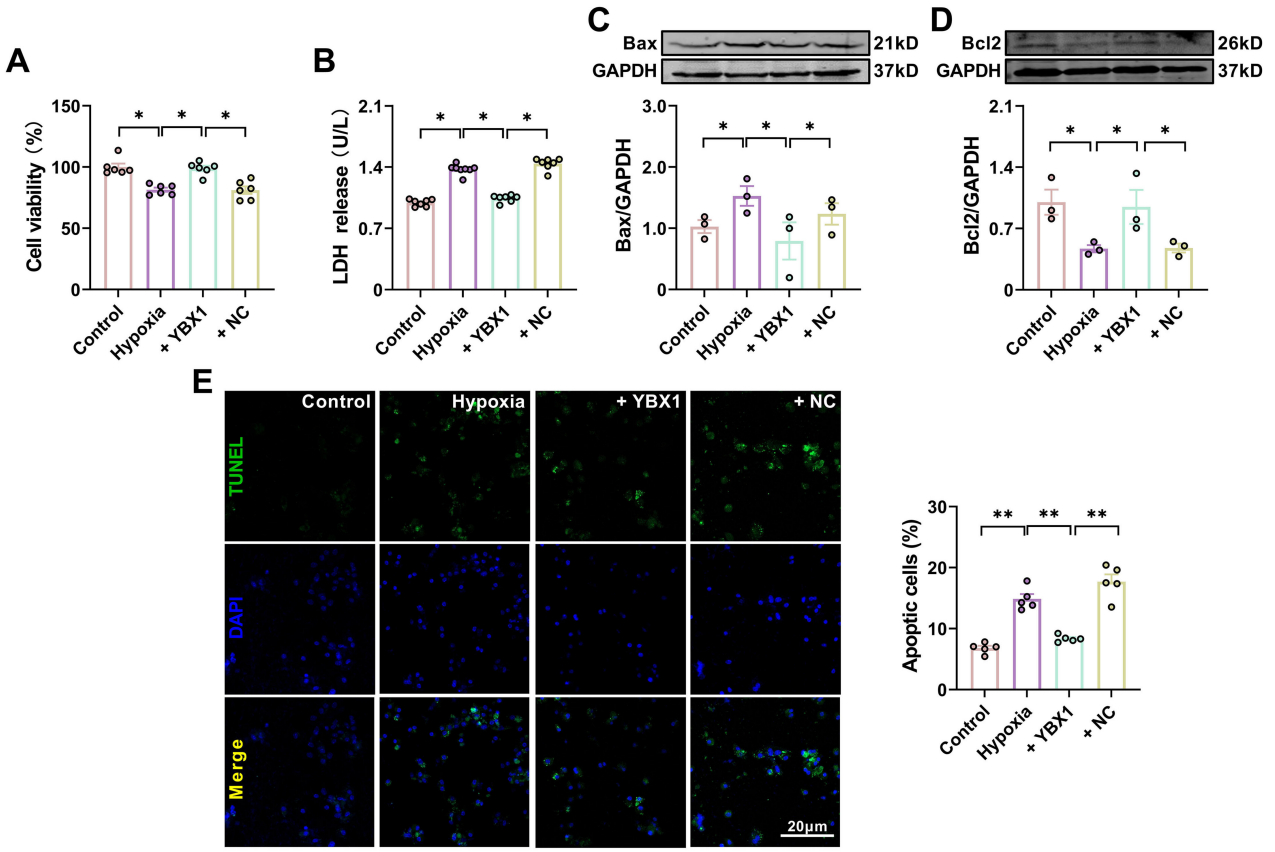

Fig. 4 YBX1 suppresses cardiomyocyte apoptosis induced by hypoxia. (A) Viability of cardiomyocytes. $^{*}P < 0.05$, $N = 6$ duplicates/group. (B) LDH content. $^{*}P < 0.05$, $N = 7$ duplicates/group. (C, D) Representative Western blot bands and statistical data on Bax and Bcl-2 expression in NMCMs. $^{*}P < 0.05$, $N = 3$ duplicates/group. (E) TUNEL photomicrographs of cardiomyocytes. Scale bar: 20 μm; $^{**}P < 0.01$, $N = 5$ duplicates/group. The data are presented as mean ± SEM.

dehydrogenase (LDH) in NMCMs. Overexpression of YBX1 restored cell viability and inhibited the release of LDH (Fig. 4B and 4C). In addition, the expression of Bax increased significantly whereas that of Bcl-2 decreased in the hypoxia group. Overexpression of YBX1 restored cell viability and expression of Bcl-2 (Fig. 4A and 4D), suppressing the release of LDH and the expression of Bax (Fig. 4B and 4C). Consistently, YBX1 overexpression partially reversed the increased number of TUNEL positive cells induced by hypoxia in Fig. 4E.

Aspartate proteases (caspases), a family of cysteine-dependent proteases, play an important role in the initiation and execution of apoptosis. The automatic catalytic activation of apoptosis initiation factors (caspase -2, -8, -9 and -10) triggers apoptosis and activates apoptosis executors (caspase -3, -6 and -7), leading to cell death[20]. Overexpression of YBX1 reduced the expression of cleaved-caspase-9 and cleaved-caspase-3 in NMCMs induced by hypoxia (Figure 5A and 5B). Mitochondrial dysfunction during MI is a critical determinant of cell death[3,21]. Therefore, we evaluated mitochondrial function using JC-1 staining and quantified the production of ROS and ATP. Hypoxia decreased ATP content and depolarized mitochondrial membrane potential, but increased ROS accumulation. Overexpression of YBX1 increased ATP content (Fig. 5C), decreased ROS accumulation, and hyperpolarized mitochondrial membrane potential, abrogating the mitochondrial dysfunction induced by hypoxia (Fig. 5D and 5E).

3.4 Silencing YBX1 aggravates mitochondria-dependent apoptosis in cardiomyocytes under hypoxia

Silencing YBX1 by siYBX1 (Supplemental Fig. 5) aggravated the decreased cardiomyocyte viability and increased LDH content in NMCMs exposed to hypoxia, while NC had no effect (Fig. 6A and 6B). Compared to the hypoxia group, silencing YBX1 aggravated hypoxia-induced cardiomyocyte apoptosis, as evidenced by the increased number of TUNEL positive cells (Fig. 6E) and

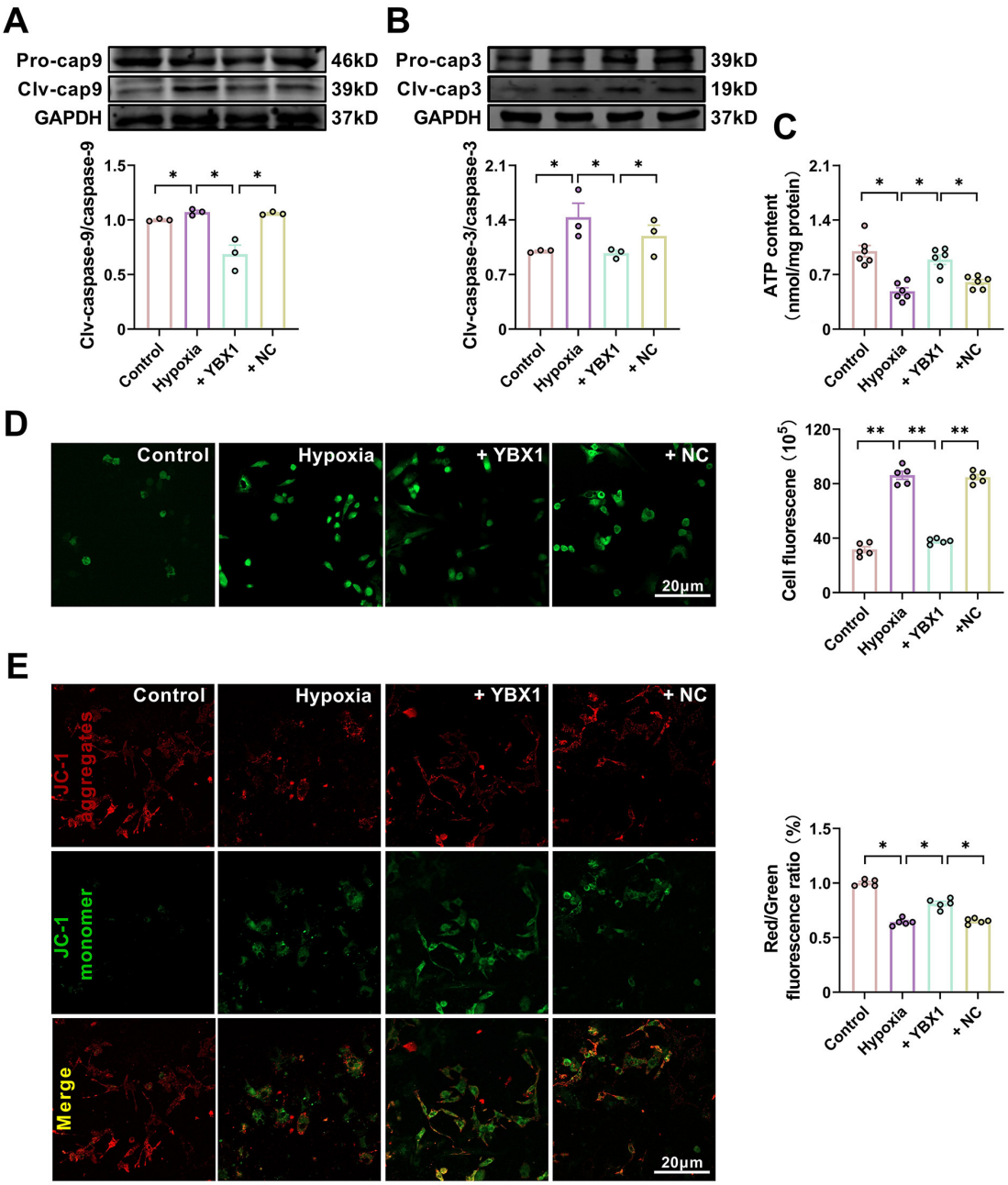

Fig. 5 YBX1 preserves mitochondrial function in neonatal mouse cardiomyocytes (NMCMs) under hypoxic conditions. (A, B) Representative Western blot bands and statistical data on caspase-9 and caspase-3 expression in NMCMs. $^{*}P < 0.05$, $N = 3$ duplicates/group. (C)ATP production. $^{*}P < 0.05$, $N = 6$ duplicates/group. (D) Effects of YBX1 overexpression on ROS production. $^{**}P < 0.01$, $N = 6$ duplicates/group. (E) Representative images of JC-1 staining for changes in mitochondrial membrane potential in NMCMs. $^{*}P < 0.05$, $N = 5$ copies/group. The data are expressed as mean ± SEM.

Bax expression levels, as well as the downregulated Bcl-2 expression (Fig. 6C and 6D). Silencing YBX1 further upregulated the protein levels of clv-caspase-9 and clv-caspase-3 under hypoxia (Fig. 7A and 7B). Silencing YBX1 reduced ATP content (Fig. 7C), increased ROS production (Fig. 7D), and depolarized mitochondrial membrane (Fig. 7E) in hypoxic NMCMs. These results indicate that YBX1 inhibits apoptosis and maintains mitochondrial function in hypoxic conditions.

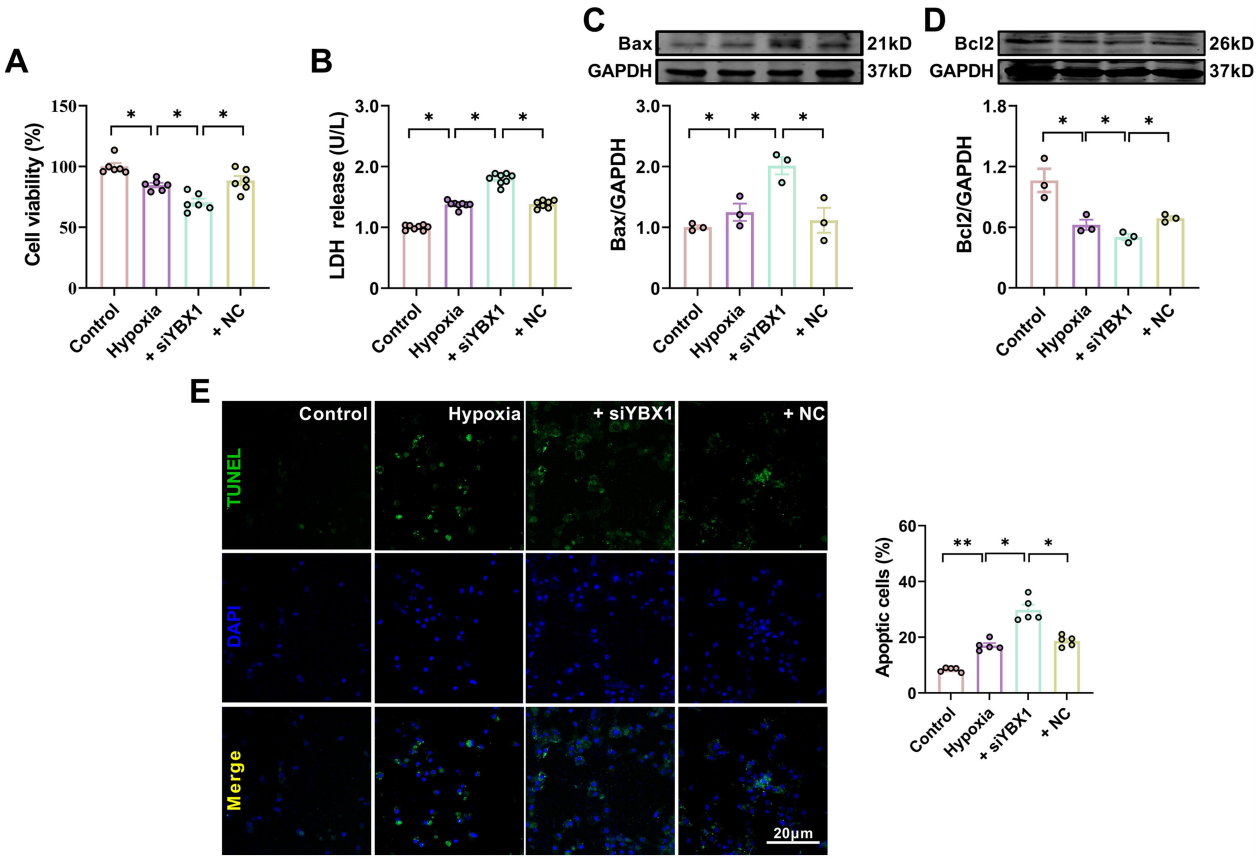

Fig. 6 Silencing YBX1 aggravates hypoxia-induced cardiomyocyte apoptosis. (A) Viability of cardiomyocytes. $^{*}P < 0.05$, $N = 6$ duplicates/group. (B) LDH release. $^{*}P < 0.05$, $N = 8$ duplicates/group. (C, D) Representative Western blot bands and statistical data on Bax and Bcl-2 expression in NMCMs. $^{*}P < 0.05$, $N = 3$ duplicates/group. (E) Typical images of TUNEL staining of cardiomyocytes. Scale bar: 20 μm; $^{*}P < 0.05$, $^{**}P < 0.01$, $N = 5$ duplicates/group. The data are presented as mean ± SEM.

3.5 YBX1 protects cardiac function through the phosphatidylinositol 3 kinase (PI3K)/AKT pathway

Data obtained from our RNA sequencing and analysis of KEGG were further analyzed using bioinformatics. The analysis indicated that the PI3K/AKT pathway is likely involved in the cardiac protective effects of YBX1 (Fig. 8A and 8B). The PI3K/AKT pathway plays an important role in various physiological and pathological processes, such as cell proliferation, metabolism, neuroprotection, and cardiac protection[22]. Moreover, correlation analysis revealed a positive correlation between YBX1 expression and the PI3K/KAT pathway, indicating that PI3K/AKT is involved in the heart protection produced by YBX1 (Fig. 8C). Overexpression of YBX1 restored the phosphorylation levels of PI3K and AKT. Compared with hypoxia group, the protein levels of PI3K and AKT in YBX1 overexpression group recovered partially to control group respectively, suggesting an activation of PI3K/AKT signal pathway (Fig. 8D and 8E). Then, we pretreated NMCMs with LY294002, an PI3K/AKT inhibitor, prior to YBX1 overexpression. LY294002 eliminated the beneficial effects of YBX1, decreasing cell viability and increasing LDH release (Fig. 8F and 8G). Additionally, LY294002 increased the expression of Bax but decreased that of Bcl-2 (Fig. 8H and 8I) and the number of TUNEL positive cells (Fig. 8J). These results suggest that PI3K/AKT is involved in the cardioprotection produced by YBX1.

4 Discussion

In this study, we initially observed that YBX1 plays a protective role in the heart against ischemic injury. This conclusion is supported by several key findings: (1) YBX1 expression was down-regulated in infarcted hearts and in hypoxic NMCMs, suggesting its involvement in ischemic conditions. (2) YBX1 improved cardiac function by inhibiting apoptosis in MI mice. (3) In NMCMs, YBX1 significantly inhibited mitochondria-dependent apoptosis and preserved mitochondrial function. (4) The protective effect of YBX1 against cardiomyocytes apoptosis was mediated through the activation of the PI3K/AKT pathway. These findings

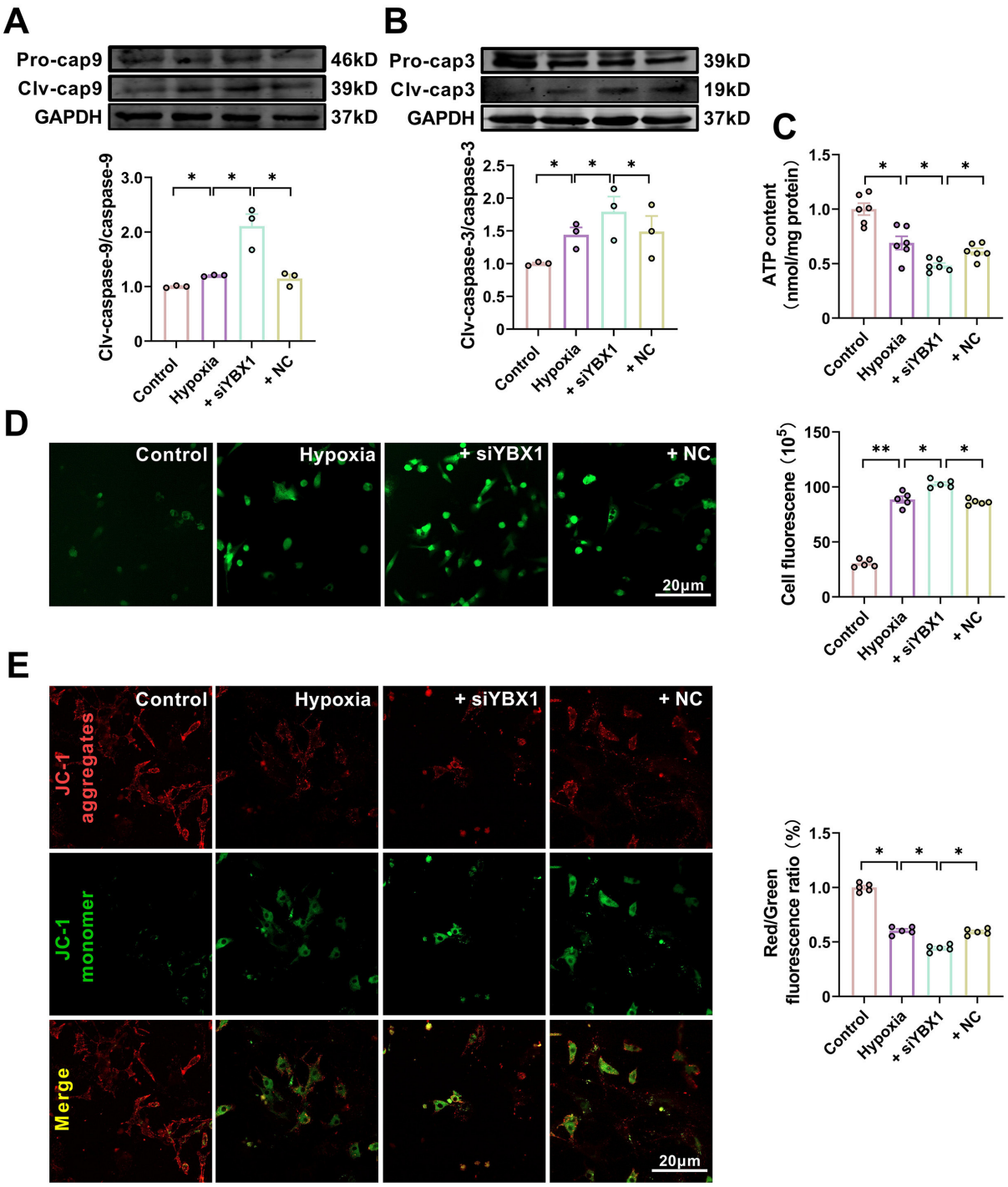

Fig. 7 Knockdown of YBX1 aggravates mitochondrial dysfunction in hypoxic neonatal mouse cardiomyocytes (NMCMs). (A, B) Representative Western blot bands and statistical data on caspase-9 and caspase-3 expression in NMCMs. $^{*}P < 0.05$, $N = 3$ duplicates/group. (C) ATP production. $^{*}P < 0.05$, $N = 6$ duplicates/group. (D) Effects of YBX1 overexpression on ROS production. $^{*}P < 0.05$, $^{**}P < 0.01$, $N = 6$ duplicates/group. (E) Representative images of JC-1 staining in NMCMs. $^{*}P < 0.05$, $N = 5$ copies/group. The data are expressed as mean ± SEM.

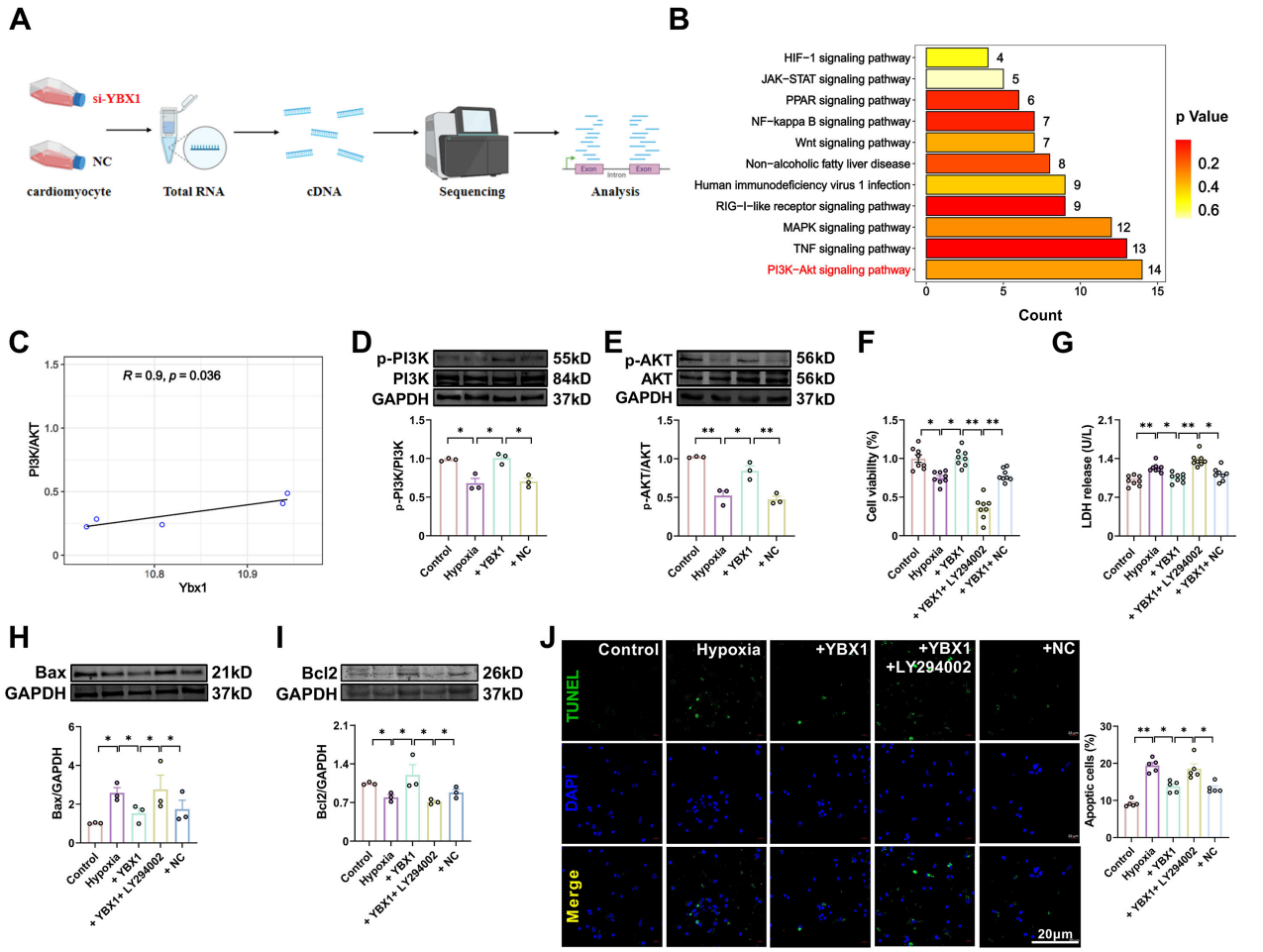

Fig. 8 YBX1 inhibits cardiomyocyte apoptosis *via* the PI3K/AKT pathway. (A, B) KEGG pathway enrichment analyses on downregulated genes in NMCMs transfected with si-YBX1 relative to control cells. (C) Correlation between YBX1 and PI3K/AKT expressions. (D, E) Representative bands and statistical data on PI3K and AKT expression, as determined by Western blot analysis. The data are presented as fold changes normalized to the sham values. $^{*}P < 0.05$, $^{**}P < 0.01$, $N = 3$ duplicates/group. (F) Viability of cardiomyocytes. $^{*}P < 0.05$, $^{**}P < 0.01$, $N = 8$ duplicates/group. (G) LDH release. $^{*}P < 0.05$, $^{**}P < 0.01$, $N = 8$ duplicates/group. (H, I) Representative bands and statistical data on Bax and Bcl-2 expression, as determined by Western blot analysis. The data are presented as fold changes normalized to the sham values. $^{*}P < 0.05$, $N = 3$ duplicates/group. (J) TUNEL assay for investigating the effect of YBX1 on apoptosis. Scale bar: 20 μm; $^{*}P < 0.05$, $^{**}P < 0.01$, $N = 5$. The data are expressed as mean ± SEM.

shed light on the potential regulatory mechanisms of YBX1 in myocardial infarction.

RNA-protein interactions are crucial for regulating cardiac function. YBX1, as an RNA-binding protein, plays a role in pathologic cardiomyocyte growth by regulating cell growth and protein synthesis. Previous research has primarily focused on the role of YBX1 during cardiac hypertrophy and cardiomyocytes regeneration. However, YBX1 as a separate RNA-binding protein that regulates the signaling cascade of cardiomyocytes during myocardial infarction remains largely unknown.

We found that YBX1 expression was down-regulated in MI mice, suggesting its potential involvement in the pathological development of MI. Overexpression of YBX1 improved the cardiac function, reduced the infarct size of MI mice, and reversed the changes in apoptotic protein levels induced by MI. Previous studies have reported contradictory results regarding the role of YBX1 in cardiac hypertrophy, with some suggesting a promoting role and others suggesting a protective role[23]. These discrepancies may be attributed to different downstream pathways activated by YBX1.

Cold exposure can induce various cellular effects, including decreases in oxygen consumption and metabolic rate[24]. Some studies have shown that cold exposure increases the ratio of

Bcl-2/Bax in the liver of mice, promoting apoptosis[25-26]. Our study showed that YBX1 increased the expression of Bcl-2 and decreased the expression of Bax, leading to reduced cardiomyocyte apoptosis. Meanwhile, YBX1 inhibited the activation of caspase-3 and caspase-9, further decreasing apoptosis. This study is the first to demonstrate the protective effect of YBX1 on myocardial infarction by inhibiting apoptosis.

YBX1 is known to regulate the physiological function of mitochondria[29-30], with its deletion in cells resulting in increased mitochondrial DNA mutation and decrease mitochondrial repair efficiency[31]. Consistent with these findings, our study showed that YBX1 overexpression maintained mitochondrial function by increasing ATP content and inhibiting ROS production induced by hypoxia. At the cellular level, YBX1 is involved in various cellular functions, including proliferation, differentiation, apoptosis, stress response, and malignant transformation. Our study found that YBX1 inhibited apoptosis in hypoxic cardiomyocytes by affecting apoptosis-related genes such as Bax, Bcl-2, caspase-9, and caspase-3, thereby maintaining mitochondrial function.

The PI3K/AKT signaling pathway regulates numerous cellular functions and is involved in preventing apoptosis in ischemic damage[36]. Our results suggest that YBX1 inhibited mitochondria-dependent apoptosis of cardiomyocytes by activating the PI3K/AKT pathway, thereby protecting the heart from ischemic damage. The PI3K inhibitor LY294002 abolished the anti-apoptotic effect of YBX1 in hypoxic NMCMs. This research provides the first evidence that YBX1 inhibits mitochondrial apoptosis by activating the PI3K/AKT pathway (Fig. 9).

5 Conclusion

In conclusion, our findings demonstrate that YBX1 activates the phosphorylation of PI3K/AKT and inhibited mitochondria-dependent apoptosis through the PI3K/AKT pathway. Myocardial infarction has become a potential therapeutic target for YBX1, and regulating the expression or activity of YBX1 may provide a new molecular strategy for the treatment of this disease.

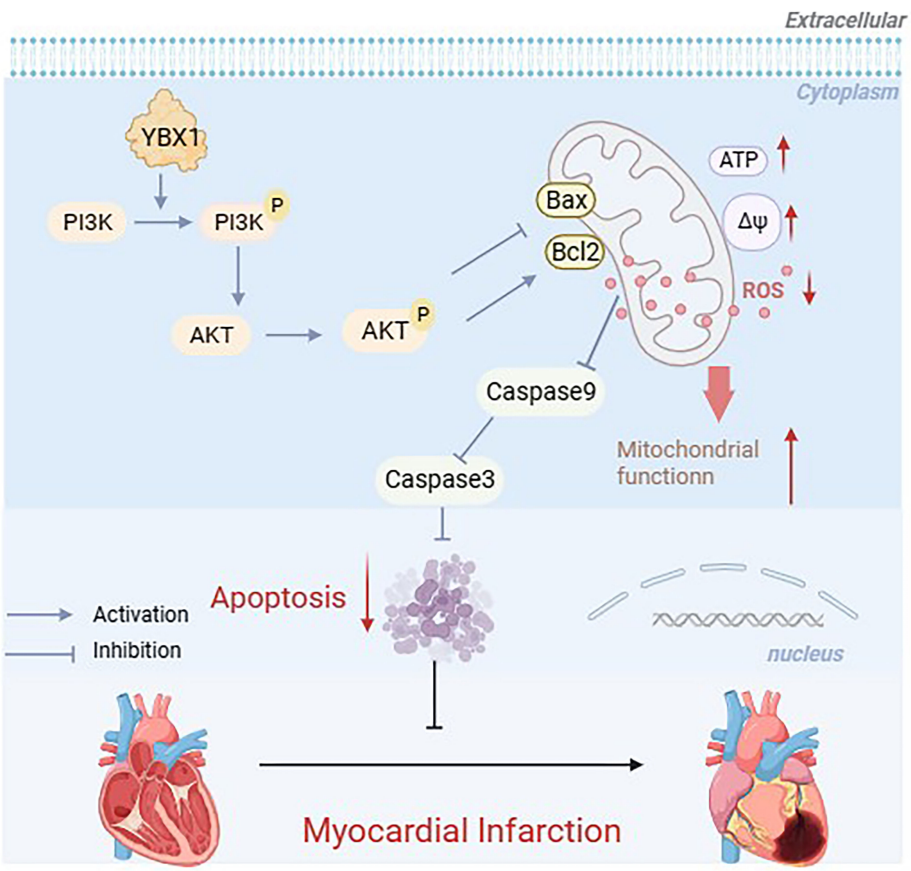

Fig. 9 Schematic diagram depicting the protective mechanisms of YBX1 in myocardial infarction. YBX1 activates PI3K/AKT phosphorylation and inhibits the mitochondria dependent apoptosis.

Author contributions

All authors contributed to the study conception and design. Material preparation, data collection and analysis were performed by Bi F F and Cao M. Project administration and methodology were performed by Wang Y Q, Pan Q M, Jing Z H, Bing D Y, Yu T, Li T Y, Lyu L F. The first draft of the manuscript was written by Zhou Y H and writing - reviewing was done by Li X L, Liang H H and Shan H L. All authors commented on previous versions of the manuscript. All authors read and approved the final manuscript.

Source of funding

This project was supported by Science and technology project of Xiamen Medical College (K2023-08), the National Natural Science Foundation of China (No.82170299 to Shan Hongli, No.82003757 to Lyu Lifang).

Ethics approval

All protocols for animal experiments were approved by the Committee for Animal Experimentation of Harbin Medical University (approval ID: DEC6121) and were conducted in accordance with NIH guidelines regarding animal experimentation.

Conflict of interests

The authors have no relevant financial or non-financial interests to disclose.

Data availability statement

The vast majority of the data generated or analyzed during this study are included in this published article and its supplementary information file. Any remaining data for the current study is available from the corresponding author(s) on reasonable request.

References

[1] Yuan X, Pan J, Wen L, *et al.* MiR-144-3p enhances cardiac fibrosis after myocardial infarction by targeting PTEN. Front Cell Dev Biol, 2019; 7: 249.
[2] Acharya D. Predictors of outcomes in myocardial infarction and cardiogenic shock. Cardiol Rev, 2018; 26(5): 255-266.
[3] Bai X, Yang C, Jiao L, *et al*. LncRNA MIAT impairs cardiac contractile function by acting on mitochondrial translocator protein TSPO in a mouse model of myocardial infarction. Signal Transduct Target Ther, 2021; 6(1): 172.
[4] Luo Y, Zhang Y, Han X, *et al.* Akkermansia muciniphila prevents cold-related atrial fibrillation in rats by modulation of TMAO induced cardiac pyroptosis. EBioMedicine, 2022; 82: 104087.
[5] Lewington S, Li L, Sherliker P, *et al.* Seasonal variation in blood pressure and its relationship with outdoor temperature in 10 diverse regions of China: the China Kadoorie Biobank. J Hypertens, 2012; 30(7): 1383-1391.
[6] Brennan P J, Greenberg G, Miall W E, *et al.* Seasonal variation in arterial blood pressure. Br Med J (Clin Res Ed), 1982; 285(6346): 919-923.
[7] Dong Y, Chen H, Gao J, *et al.* Molecular machinery and interplay of apoptosis and autophagy in coronary heart disease. J Mol Cell Cardiol, 2019; 136: 27-41.
[8] Elsässer A, Suzuki K, Lorenz-Meyer S, *et al.* The role of apoptosis in myocardial ischemia: a critical appraisal. Basic Res Cardiol, 2001; 96(3): 219-226.
[9] Slee E A, Adrain C, Martin S J. Serial killers: ordering caspase activation events in apoptosis. Cell Death & Differentiation, 1999; 6(11): 1067-1074.
[10] Jose Corbalan J, Vatner D E, Vatner S F. Myocardial apoptosis in heart disease: does the emperor have clothes? Basic Res Cardiol, 2016; 111(3): 31.
[11] Suresh P S, Tsutsumi R, Venkatesh T. YBX1 at the crossroads of non-coding transcriptome, exosomal, and cytoplasmic granular signaling. Eur J Cell Biol, 2018; 97(3): 163-167.
[12] Cui Q, Wang C, Liu S, *et al.* YBX1 knockdown induces renal cell carcinoma cell apoptosis *via* Kindlin-2. Cell cycle (Georgetown, Tex.), 2021; 20(22): 2413-2427.
[13] Zhang H, Zheng W, Li D, *et al.* MiR-379-5p promotes chondrocyte proliferation *via* inhibition of PI3K/Akt Pathway by targeting YBX1 in osteoarthritis. Cartilage, 2022; 13(1): 19476035221074024.
[14] Hussain S A, Venkatesh T. YBX1/lncRNA SBF2-AS1 interaction regulates proliferation and tamoxifen sensitivity *via* PI3K/AKT/MTOR signaling in breast cancer cells. Molecular Biology Reports, 2023; 50(4): 3413-3428.
[15] Lin F, Zeng Z, Song Y, *et al*. YBX-1 mediated sorting of miR-133 into hypoxia/reoxygenation-induced EPC-derived exosomes to increase fibroblast angiogenesis and MEndoT. Stem Cell Res Ther, 2019; 10(1): 263.
[16] Huang S, Li X, Zheng H, *et al.* Loss of super-enhancer-regulated circRNA nfix induces cardiac regeneration after myocardial infarction in adult mice. Circulation, 2019; 139(25): 2857-2876.
[17] Pham T P, Bink D I, Stanicek L, *et al.* Long Non-coding RNA Aerrie Controls DNA Damage Repair *via* YBX1 to Maintain Endothelial Cell Function. Front Cell Dev Biol, 2020; 8: 619079.
[18] Varma E, Burghaus J, Schwarzl T, *et al.* Translational control of Ybx1 expression regulates cardiac function in response to pressure overload *in vivo*. Basic Res Cardiol, 2023; 118(1): 25.
[19] Jing X, Yang F, Shao C, *et al.* Role of hypoxia in cancer therapy by regulating the tumor microenvironment. Mol Cancer, 2019; 18(1): 157.

[20] Zamaraev A V, Kopeina G S, Prokhorova E A, *et al.* Post-translational Modification of Caspases: The Other Side of Apoptosis Regulation. Trends Cell Biol, 2017; 27(5): 322-339.
[21] Ramachandra C J A, Hernandez-Resendiz S, Crespo-Avilan G E, *et al.* Mitochondria in acute myocardial infarction and cardioprotection. EBioMedicine, 2020; 57: 102884.
[22] Glaviano A, Foo A S C, Lam H Y, *et al.* PI3K/AKT/mTOR signaling transduction pathway and targeted therapies in cancer. Mol Cancer, 2023; 22(1): 138.
[23] Yang R, Li L, Hou Y, *et al.* Long non-coding RNA KCND1 protects hearts from hypertrophy by targeting YBX1. Cell Death Dis, 2023; 14(5): 344.
[24] Sepa-Kishi D M, Sotoudeh-Nia Y, Iqbal A, *et al.* Cold acclimation causes fiber type-specific responses in glucose and fat metabolism in rat skeletal muscles. Sci Rep, 2017; 7(1): 15430.
[25] Liu P, Yao R, Shi H, *et al.* Effects of cold-inducible RNA-binding Protein (CIRP) on liver glycolysis during acute cold exposure in C57BL/6 mice. Int J Mol Sci, 2019; 20(6): 1470.
[26] Xu B, Lang L M, Li S Z, *et al.* Cortisol excess-mediated mitochondrial damage induced hippocampal neuronal apoptosis in mice following cold exposure. Cells, 2019; 8(6): 612.
[27] Kloetgen A, Duggimpudi S, Schuschel K, *et al.* YBX1 indirectly targets heterochromatin-repressed inflammatory response-related apoptosis genes through regulating CBX5 mRNA. Int J Mol Sci, 2020; 21(12): 4453.
[28] Su H, Fan G, Huang J, *et al.* YBX1 regulated by Runx3-miR-148a-3p axis facilitates non-small-cell lung cancer progression. Cell Signal, 2021; 85: 110049.
[29] David J J, Subramanian S V, Zhang A, *et al.* Y-box binding protein-1 implicated in translational control of fetal myocardial gene expression after cardiac transplant. Experimental Biology & Medicine, 2012; 237(5): 593-607.
[30] Ma L, Singh J, Schekman R. Two RNA-binding proteins mediate the sorting of miR223 from mitochondria into exosomes. Elife, 2023; 12: e85878.
[31] Kishikawa T, Otsuka M, Yoshikawa T, *et al.* Satellite RNAs promote pancreatic oncogenic processes *via* the dysfunction of YBX1. Nat Commun, 2016; 7: 13006.
[32] Feng M, Xie X, Han G, *et al.* YBX1 is required for maintaining myeloid leukemia cell survival by regulating BCL2 stability in an m6A-dependent manner. Blood, 2021; 138(1): 71-85.
[33] Chen J, Liu Z, Zhang H, *et al.* YBX1 promotes MSC osteogenic differentiation by activating the PI3K/AKT pathway. Curr Stem Cell Res Ther, 2023; 18(4): 513-521.
[34] Tuerxun T, Li X, Lou F, *et al.* YBX1 protects against apoptosis induced by oxygen-glucose deprivation/reoxygenation in PC12 cells *via* activation of the AKT/GSK3β pathway. Folia Biol (Praha), 2021; 67(4): 150-157.
[35] Su W, Wang L, Zhao H, *et al.* LINC00857 interacting with YBX1 to regulate apoptosis and autophagy *via* MET and phosphor-AMPKa signaling. Mol Ther Nucleic Acids, 2020; 22: 1164-1175.
[36] Wang J, Hu K, Cai X, *et al.* Targeting PI3K/AKT signaling for treatment of idiopathic pulmonary fibrosis. Acta Pharm Sin B, 2022; 12(1): 18-32.
[37] Liu C, Chen K, Wang H, *et al.* Gastrin attenuates renal ischemia/reperfusion injury by a PI3K/Akt/Bad-mediated anti-apoptosis signaling. Front Pharmacol, 2020; 11: 540479.
[38] Feng C, Wan H, Zhang Y, *et al.* Neuroprotective effect of danhong injection on cerebral ischemia-reperfusion injury in rats by activation of the PI3K-Akt pathway. Front Pharmacol, 2020; 11: 298.
[39] Li Y, Xia J, Jiang N, *et al.* Corin protects H(2)O(2)-induced apoptosis through PI3K/AKT and NF-κB pathway in cardiomyocytes. Biomed Pharmacother, 2018; 97: 594-599.
[40] Chen R, Chen T, Wang T, *et al.* Tongmai Yangxin pill reduces myocardial no-reflow by regulating apoptosis and activating PI3K/Akt/eNOS pathway. J Ethnopharmacol, 2020; 261: 113069.